

# Exploration of Ion Sensitive Field-Effect Transistor With Dielectric Properties

Abhishek Kumar

Lovely Professional University

Suman Lata Tripathi (✉ [tri.suman78@gmail.com](mailto:tri.suman78@gmail.com))

Lovely Professional University <https://orcid.org/0000-0002-1684-8204>

---

## Research Article

**Keywords:** ISFET, BioFET, Electrolyte, Dielectric, Bio-sensor, Electrochemical

**Posted Date:** May 10th, 2021

**DOI:** <https://doi.org/10.21203/rs.3.rs-447250/v1>

**License:**   This work is licensed under a Creative Commons Attribution 4.0 International License.

[Read Full License](#)

---

# Abstract

Environmental changes and increased virus effects in COVID-19 like the situation is forcing the design and researchers to develop highly sensitive, low power and low cost mean to detect the presence of biomolecules of different shapes, sizes, and their effects on the human being. Ion-sensitive field-effect transistor (IS-FET) is a biological sensor based on the architecture of metal oxide semiconductor field-effect transistor (MOS-FET). The gate terminal is replaced with a hollow space filled by electrolyte solution and reference electrode at the external surface. The biomolecular enzyme in contact with membrane enters in solution induce net DC potential, alter the oxide surface. The alteration of surface puts variation in threshold voltage and maps on the deflection of drain current. ISFET measures the concentration of charged particles (ions) in the solution; variation into ion concentration produces deflection in the drain current. In this work numerical simulation of ISFET is performed with ENBIOS-2D Lab at Nanohub platform with dielectric  $\text{SiO}_2$ ,  $\text{Al}_2\text{O}_3$ ,  $\text{HfO}_2$  with NaCl and KCl in solution. Channel resistance and capacitance with 3-different electric shows a large variation of capacitance, result in threshold voltage i.e. 318.2 mV with  $\text{SiO}_2$  and 319.2 mV with  $\text{Al}_2\text{O}_3$ .

## Introduction

Chemical sensor research based on Ion-sensitive field-effect transistor (ISFET) is dynamic in the area of environmental monitoring application, biomedical molecule, analytical chemistry, and pharmaceutical testing since invented by P. Bergveld [1] in 1972. It works as a biological electronics interface; architecture is similar to the existing metal-oxide field-effect transistor (MOSFET), the only difference lies in terms of gate terminal. In MOSFET gate electrodes are in contact with the oxide dielectric layer while in ISFET the oxide dielectric is in contact with the reference electrode via electrolyte solution [2]. ISFET is 3 terminal devices; source, drain, gate presented in Fig. 1 consist of a combination of biological elements and a semiconducting transducer layer [3]. Stable reference electrodes are placed to set the constant gate surface potential. The conduction layer is similar to the conventional field-effect transistor; the functionality of the dielectric layer is understood as isolation of channel and coupling of bimolecular charges to the channel. A bio-functionalized layer exhibits an immobilized bimolecular charge known as a receptor on the top of the dielectric [4].

Sensing of biological signals with FET devices drew attention due to its excellent sensing properties and effective cost. Conventional FET devices establish the flow of current between sources and drain terminal under the influence of electric field produces by potential applied at 3rd gate terminal, whereas in ISFET gate electrode are in the contact of the electrolytic solution. The gate surface must bio-functionalized with receptor molecule that gets capture into the FET gate surface result in the variation of its surface potential. Due to the variation of charge, it affects the measurable drain to source current [5]. It senses the biomedical signal and integrates the amplifying device on the chip itself. The sensing of bio-molecular detection is based on NMOS, a biotin-streptavidin complex chosen for the modeling due to purification and delectability [6]. The presence of ion particles creates DC potential in the solution. Biasing of ISFET induces, energy barrier, doesn't remain the constant between Fermi level and oxide breakdown, the

distinction between valance electron level of the conduction particle species in the electrolyte and oxide conduction band.

The ability of ISFET to sense the living cell attracts the researcher to reads the biological information [7], majorly find application in drug screening, sensing the biochemical compound, and study of neural network. It ensures pH and other electrolyte solutions, exposed to the dielectric to the electrolyte acts as a biological FET (BioFET) based sensor. The biological sensor field-effect transistor is a combination of sensitive biological recognition elements and is the FET that can detect the antigen in the body and tumor markers. BioFET measures the change in surface potential induced by binding of the molecule when the bimolecular binds with the gate terminal (a dielectric material). A pH-sensitive oxide layer in contact with electrolyte solution under biased condition, variation in pH value is detected which is measure by variation in drain current [8]. DC Current in electrolyte-oxide-semiconductor (EOS) is accompanied by electrolysis which is visualized by the production of gas at the electrode. Higher drain to source potential  $V_{DS}$  holes repeal from source terminal, create a conduction channel of the hole. The charged particle directed towards gate oxide (x-direction) potential varies with distance concerning the reference electrode. Maximum alternation found near the oxide interface receptor which varies the resistance and capacitance of the channel behind the dielectric. If the target molecule is a positively charged n-type FET sensor is the upsurge in the conductance because of the presence of electrons, conversely if the target molecule is negatively charged the p-type FET upsurge in the resistance because of holes. The flow of carrier is controlled by gate voltage  $V_{GS}$ , the number of charge carrier in the channel, influence the conductance and resistance of the channel consequently affect the drain current  $I_{DS}$ . The charge induces in the channel due to the capacitive effect of the dielectric layer with a constant  $k$  value between the gate electrode and channel.

A thin oxide layer between sources to drain terminal as gate oxide is used to produce carrier in the channel. Another gate-source voltage  $V_{GS}$  applied to gate oxide via the electrolyte controls the conduction of the carrier into the channel upon creation of inversion layer at threshold voltage ( $V_T$ ). A voltage-current characteristic presents relation; at  $V_{GS} = 0$  and  $V_{DS} > 0$ ;  $I_{DS} = 0$  a small leakage current flow due to reverse bias of PN junction. When  $V_{GS} > 0$  the carrier from the source attracts toward the drain terminal due to the effect of the electric field of  $V_{GS}$ , the charge appears in the central region and creates an inverted channel. These inversion channels present the area where the carrier flows, under this situation drain begins to flow. When  $V_{GS} > V_T$  a large linear increase in  $I_{DS}$  increases linearly.  $I_{DS}$  increases with  $V_{DS}$  however  $V_{DS} > V_{GS} - V_T$  inversion channel shortens, and  $I_{DS}$  enters into saturation region. The drain to source resistance compensates by a shortened inversion channel at higher  $V_{DS}$ . Finally,  $I_{DS}$  saturates become constant and independent.

The electrical readout of ISFET is the drain to source voltage proportional to the pH concentration of the electrolyte as presented in [9, 10]. A biological enzyme enters the solution reacts with salt and frees the ion, electrons, and holes. Hydrogen ion concentration controls the drain to source current, pH solution contains  $H^+$  ion. A higher concentration of  $H^+$  ion has a low pH value and vice versa. Positive charge ions

produce electrical potential by way to diffuse through the membrane at oxide layer, tends to except  $H^+$  ion requires additional gate voltage to maintain constant threshold voltage to create a channel between source to drain. The selectivity and sensitivity of ISFET highly depend on the selection of gate and sensitivity of the surface of dielectric material [11–13].  $I_{DS}$  depends on the potential difference over gate oxide, influenced by the oxide-electrolyte solution.

In this work, the dielectric layer experimented with different materials  $SiN_4$ ,  $Al_2O_3$ ,  $Ta_2O_5$ ,  $SiO_2$  which acts independently to  $H^+$  ions. The biological analytes in the solution decrease the binding and enable the charge transfer to the surface of the transducer chemically or electrostatic interaction. During the interaction between membrane and target variation in the oxide surface seen which turn in the change in conductivity of channel, by measuring the change the binding of the analyte can be detected [14]. Section 2 discusses the surface potential induces by the reference electrode and gate oxide. Simulation results obtained with nanohub tool included in Sect. 3, Sect. 4 read out the variation in threshold voltage ( $V_{th}$ ) finally concluded in Sect. 5.

## Isfet As Sensor

ISFET based biosensors find commonly for the early detection of various diseases since molecules transmit electrical charges rapidly. The existing CMOS fabrication process offers the advantage of miniaturizing and concurrent sensing. Different biological analytes have experimented with for the detection of viruses including COVID-19, Influenza, and Hepatitis-B, etc, besides it also uses for designing nucleic acid sensors depends on DNA hybridization [15]. The advantage of the ISFET sensor emerges in speed, sensitivity, specificity which is the primary requirement of COVID-19 detection presented in [16]. Graphene-based FET biosensors can detect surroundings changes in their surface and provide an optimal sensing environment for low noise detection. The electrolyte solution used to cover is phosphate-buffered saline (PBS, pH = 7.4) to maintain an efficient gate electrode. Based on the charge in aqueous solution in surface potential and their effect on the electrical characteristics can detect SARS-CoV-2 spike on the surface V-I characteristics over ranges of -0.1 to + 0.1 V before and after attachment of the antibody, after immobilization of antibody on the surface the slope ( $dI/dV$ ) decreased, the difference in slope presented the introduction of SARD-CoV2 spike antibody.

### 2.1 Reference Electrode

FET structures of the biosensor are equivalent to insulated gate FET (IGFET) or ISFET. In IGFET the gate terminal is detached from the source and channel terminal while in an ISFET gate terminal is supplanted by the particle-specific film, reference electrode, and electrolyte. In ISFET the channel appeared due to an electrochemical effect[17]. In MOSFET capacitive effect is due to the dielectric layer while in ISFET capacitive effect due to the cumulative effect of the dielectric layer and capacitance of the electrical double layer (EDL). The EDL arises due to the distribution of the ion in solutions near the solid-liquid interfacing surface and exerts a capacitance known as electrical double layer capacitance (EDLC) [18]. EDLC can calculate by applying a potential in the liquid, the polarity of EDL can change by bias voltage in

the solution. ON and the OFF state of ISFET can relate as presence and absence of charge carrier in the channel presented in Fig. 2. A reference electrode usually (Ag or AgCl) used to apply the bias voltage in the solution. Charge molecule on the surface and binding of analyte molecules produces a change in the surface charge result in a change in the effective gate voltage needed to turn ISFET ON/OFF. The current flow not only due to the charges of bimolecular interacting on gate electrode but also sensitive to pH of fluid, different ions, enzyme reaction[19]

Biological sensitive FET is highly sensitive to select the biomedical or chemical analyte due to the bio-recognition layer at the surface. The performance of a biosensor depends on the selection of a bio-recognition layer. These layers provide specific interaction with molecules, binding, and charge transfer. The electrical detection of biomolecules in the solution follows a different strategy. A small charged molecule in a low ionic solution needed potentiometric readout. pH-sensitive array-based Biosensor, remove the metal gate from top and passivation layer is deposited. This layer creates additional capacitance in series; which limits the sensitivity [20] ISFET based sensing application requires a stable reference electrode, and indistinguishable from a change in detectable chemical potential. Ag/AgCl element in the membrane covers within  $\pm 0.5$  mV in 0.1 M in the mixture of NaCl or KCl solution. RC model at the electrode reveals the ion to electron conduction principle at the reference electrode by redox reaction [20].



Redox sensitive material at the reference electrodes measures capacitance C while current i flow through electrode voltage v, a small resistance exhibit that shifts the potential, described miniaturization of reference electrode increase the resistance and decrease in capacitance [21].

$$\frac{\Delta V}{\Delta i} = \frac{i}{c} \quad \text{and} \quad \Delta v = iR \quad (2)$$

The passivation layer for sensing creates variation in the threshold due to charge trap in the layer[21] The resulting sensors are highly successful in pH measurement. The reduction in threshold voltage is measured by Eq. (1)

$$V_{TH(ISFET)} = V_{TH(MOSFET)} - V_{CHEMICAL} \quad (3)$$

$$V_{CHEMICAL} = E_i + \frac{RT}{\eta F} \ln(a) \quad (4)$$

Where  $V_{CHEMICAL}$  is the voltage induced by electrochemical process,  $E_i$  is chemical constant, F is Faraday constant, T is the temperature in kelvin, R is gas constant,  $a_i$  is the activity of ion, and  $\eta$  is ion charge [22]

## 2.2Oxide surface potential

For 30 years several fabrication methodologies for ISFET sensors have been proposed with different materials. The processing equipment of ISFET fabrication is common with integrated technology (IC) technologies fabrication. Fabrication begins with, < 100 > p-type semiconductor as substrate and heavily doped by n-type semiconductor creates source and drain terminal. The doping level ensures a low leakage current. In this work, ISFET has experimented with materials like  $\text{SiO}_2$ ,  $\text{Al}_2\text{O}_3$ , and  $\text{HfO}_2$  surrounded by electrolyte solution AgCl and NaCl. The oxide surface of the ISFET gate surrounded by electrolyte solution reacts with charged ion breaks the bond; result in  $\text{O}_2^+$  or  $\text{OH}^-$  group of ions. Depending on gate oxide and pH value of solution net positive or negative charge built up near the oxide surface. Site binding model [23] a charge at oxide surface due to the result of thermodynamic equilibrium between OH group of surface and  $\text{H}_3\text{O}^+$  and  $\text{OH}^-$  ion [24] models the surface reaction site of oxide and ions and get absorbed result in charge surface. The  $\text{Na}^+$  and  $\text{K}^+$  ion concentration controls the electrical activity primarily and current flow over the membrane[25–29]. The oxide surface altered due to the reaction of  $\text{Na}^+$  and  $\text{K}^+$  ions at the surface.

## Simulation Result Of Isfet

ISFET measures the pH value; consequently, results in a change of transistor current. The gate electrode is the solution and voltage between the oxide surface and substrate. ISFET based pH sensors are based on electrolyte solution. The electrolyte solutions when in contact with the solid-liquid interface possess a net surface charge which produces the effect over effective gate voltage. The carrier flows through the channel with the cumulative effect of applied gate potential and protonation and deprotonation of electrolyte solution near the surface. The FET device transforms the binding or charges concentration on the surface into the electronics signal. The simulation parameter given in [26] has been used for the simulation model used for the simulation of ISFET with an open-source tool available on the Nanohub platform. The bimolecular enzyme in contact with membrane travels towards dielectric through the solution; in this work, the experimentation with the salt of 1mM NaCl and 1mM KCl in water-electrolyte with pH value 7 has been analyzed to perform characteristics of BioFET. Movement of DC concentration of charged particle in the solution along Z-direction of FET, with dielectric  $\text{SiO}_2$ ,  $\text{Al}_2\text{O}_3$  and  $\text{HfO}_2$  has been analyzed numerically. The architecture of BioFET presented below architected with a channel length of 200 nm, source/drain length 50 nm with oxide thickness of 3 nm. 400 nm of thick oxide has been used for passivation across the source and drain region which overlaps the source and drain region by 50 nm, thus the effective area for oxide surface is 100 nm. The upper structures of FET are filled with aqueous electrolyte solution with salt with NaCl and KCl which allows the charged particle to move towards the oxide binding site. Reference electrode width 20 nm towards z-axis used for the biasing to create the channel and maintain a DC operating point (0.319 V, 25 mA/A).

Figure 3(a) and 3(b) VI characteristics of the ISFET present the variation of current per unit area in NaCl and KCl solution concerning fluid gate voltage with  $\text{SiO}_2$ ,  $\text{Al}_2\text{O}_3$ , and  $\text{HfO}_2$  dielectric. Initially current value approx to zero, channel formation begins with threshold voltage 0.319V. The slope of the current curve with NaCl salt and with KCl salt observed current increased for a higher value of dielectric. Electrolyte

solution with charged particle achieves the bias current 25 mA/m at 0.31895V, 0.31928V, and 0.31881V for SiO<sub>2</sub>, Al<sub>2</sub>O<sub>3</sub>, and HfO<sub>2</sub> dielectric. The magnitude of current increases with a high k value of the dielectric. With DC bias drain current achieves 46.4uA, 69.9uA, and 109.21uA with SiO<sub>2</sub>, Al<sub>2</sub>O<sub>3</sub>, and HfO<sub>2</sub> dielectric respectively.

Bimolecular enzyme touches the membrane reacts with salt in the solution and induces the charged particle. Movements of charged particle towards gate oxide in the z-direction (at x = 0 nm, center of the silicon film, and at z = 24 nm, i.e., one nm above the Si-Dielectric interface) presented in Fig. 4. It is observed that a negative peak occurs due to the charge built up near the site binding at the dielectric and electrolyte interface. The concentration of ions with V<sub>FG</sub>=0 V the Na<sup>+</sup> ion is higher than Cl<sup>-</sup> concentration, the difference between them creates a net positive charge in the solution, the diffusion layer is balanced negative site binding charge. The curve gets reverse for higher dielectric oxides, for Al<sub>2</sub>O<sub>3</sub> and HfO<sub>2</sub>, Na<sup>+</sup> ions are lower than Cl<sup>-</sup> thus creates a negative charge in the solution. The Concentration of 6.022\*10<sup>23</sup>/m<sup>3</sup> maintains constant potential at 219.6 nm, 415.387 nm, and 433.138 nm for SiO<sub>2</sub>, Al<sub>2</sub>O<sub>3</sub>, and HfO<sub>2</sub> dielectric respectively.

Figure 5 presents the concentration of K<sup>+</sup> and Cl<sup>-</sup> concentration of charged particles in an electrolyte solution with KCl salt at Z = 24 nm. The concentration of K<sup>+</sup> is lower than Cl<sup>-</sup> with oxide dielectric SiO<sub>2</sub> and HfO<sub>2</sub>; creates a net negative charge; while Al<sub>2</sub>O<sub>3</sub> dielectric creates a higher K<sup>+</sup> ion than Cl<sup>-</sup> concentration creates a net positive charge in the electrolyte solution. The concentration of charged particles gets saturated at 6.022\*10<sup>23</sup>/m<sup>3</sup> at 366.528 nm, 425.387 nm, and 433.138 nm for SiO<sub>2</sub>, Al<sub>2</sub>O<sub>3</sub>, and HfO<sub>2</sub> dielectric from the site bind interface.

The flow of charged particles towards the gate terminal induces DC potential. Figure 6(a) along z-direction (x = 0 nm). The maximum value of potential reaches - 31 nm i.e. inside the channel. The induced dc voltage 69.34 mV for SiO<sub>2</sub> and reduces with the higher value of dielectric; 65.5 mV for Al<sub>2</sub>O<sub>3</sub> and 61.76 mV for HfO<sub>2</sub> respectively. At the interface net, DC voltage is 35.1 mV, 32.44 mV, and 30.12 mV for SiO<sub>2</sub>, Al<sub>2</sub>O<sub>3</sub>, and HfO<sub>2</sub> respectively. The potential tend to decrease with the upward Z-axis; can be approximated to zero afterward 52 nm from oxide electrolyte interface. As enzymes in contact of membrane react with electrolyte solution free the charged particle, when their concentration reaches the significant value of 6.023\*10<sup>23</sup>/m<sup>3</sup> at a distance of 52 nm; DC potential induces 0.157 mV. DC potential along X-axis (z-direction) shown in Fig. 6(b) is minimum at the center of oxide, reaches the maximum value to both sides. DC voltage rises exponentially till z = 100 nm; reaches a maximum value of 0.575V

The variation in resistance (solid line) and capacitance (dashed line) in the channel with different dielectric is presented in Fig. 7 with AC analysis with frequency ranges 1KHz to 1GHz. At lower frequency till 46.4 MHz offers approximately equal resistance 482 ohm, however SiO<sub>2</sub> dielectric offers maximum resistance compare to the other two, this resistance increases with a higher value of K. Conversely the

capacitance is attaining minimum for SiO<sub>2</sub> and increase with a higher K value of dielectric. The channel offers the constant value of capacitance 28.8 fF till frequency 215.4 kHz then tends to fall.

## Isfet Signal Readout

ISFET maps the voltage induced by the bimolecular enzyme into the variation of the threshold voltage. Eq. (3) measures the variations of threshold voltage as the contraction of  $V_{\text{CHEMICAL}}$  induce by the electrochemical process. The variation into threshold voltage can also be reflected in the deflection of current. A constant drain current measure by employing NaCl and KCl in an electrolyte solution with different dielectric is presented in Table 1. In both types of solution, the maximum threshold voltage occurs for ISFET with Al<sub>2</sub>O<sub>3</sub> dielectric, however, the maximum shift is 0.125%. Deflection of the current value is read at constant DC potential 0.5 V; drain current measures as 3.89  $\mu$ A, 4.36  $\mu$ A, and 5.02  $\mu$ A with gate dielectric SiO<sub>2</sub>, Al<sub>2</sub>O<sub>3</sub>, and HfO<sub>2</sub>. A current amplifier usually an instrumentation amplifier at the electronic readout circuit that read the deflection of current due to the chemical voltage induced by enzymes,

Table 1  
Threshold voltage with dielectric

Dielectric	Threshold Voltage (V)
SiO <sub>2</sub>	0.3189
Al <sub>2</sub> O <sub>3</sub>	0.3192
HfO <sub>2</sub>	0.3188

## Conclusion

In this work, the detailed analysis of ISFET structure with the involvement of different dielectric as a gate oxide in an electrolyte solution with NaCl and KCl salt has been presented. Simulation result obtained with ENBIOS-2D Lab of Nanohub computes maximum variation is found with high K dielectric at the gate terminal. DC potential induced solution towards gate oxide is a maximum of 0.069 V for SiO<sub>2</sub> dielectric and 0.061736 V with HfO<sub>2</sub> dielectric. For the frequency range of 1KHz to 1GHz, the channel resistance is directly related to the K value and channel capacitance is inversely related to the K value. The high value of deflection current shows that HfO<sub>2</sub> offers low resistance in comparison to SiO<sub>2</sub> and Al<sub>2</sub>O<sub>3</sub>. The projected analysis can be extended to other available FET-based sensors such as multi-gate MOSFET or TFET architectures.

## Declarations

### Funding

There is no funding received for this work.

### **Conflicts of interest/Competing interests**

There is no conflict of interest at any stage.

### **Availability of data and material**

The associated data will be made available on request.

### **Code availability**

The simulation work has been carried out using open-source online simulator nanohub.

### **Authors' contributions** (optional): NA

The performance evaluation of Bio-FET has been covered in this work.

### ***Additional declarations***

### **Ethics approval:** NA

It is a simulation-based design and analysis. So, it does not produce any environmental hazards.

### **Consent to participate**

Yes, we are ready to participate.

### **Consent for publication**

We are ready for publication with your journal.

## **References**

1. Bergveld, P. (1970). Development of an ion-sensitive solid-state device for neurophysiological measurements. *IEEE Transactions on Biomedical Engineering*, (1), 70-71
2. Kalnitsky, A., Yi-Shao, L. I. U., Liang, K. C., Chu, C. H., Cheng, C. R., & Cheng, C. W. (2016). *S. Patent No. 9,459,234*. Washington, DC: U.S. Patent and Trademark Office.
3. Sohn, Y. S., Lee, S. K., & Choi, S. Y. (2007). Detection of C-reactive protein using BioFET and extended gate. *Sensor Letters*, 5(2), 421-424.
4. Martinoia, S., Massobrio, G., & Lorenzelli, L. (2005). Modeling ISFET microsensor and ISFET-based microsystems: a review. *Sensors and Actuators B: Chemical*, 105(1), 14-27.
5. Palan, B., Santos, F. V., Karam, J. M., Courtois, B., & Husak, M. (1999). New ISFET sensor interface circuit for biomedical applications. *Sensors and Actuators B: Chemical*, 57(1-3), 63-68.

6. Milgrew, M. J., & Cumming, D. R. (2008). Matching the transconductance characteristics of CMOS ISFET arrays by removing trapped charge. *IEEE Transactions on Electron Devices*, *55*(4), 1074-1079.
7. Shul'ga, A. A., Sandrovsky, A. C., Strikha, V. I., Soldatkin, A. P., Starodub, N. F., & El'Skaya, A. V. (1992). Overall characterization of ISFET-based glucose biosensor. *Sensors and actuators B: chemical*, *10*(1), 41-46.
8. Bandiziol, A., Palestri, P., Pittino, F., Esseni, D., & Selmi, L. (2015). A TCAD-based methodology to model the site-binding charge at ISFET/electrolyte interfaces. *IEEE Transactions on Electron Devices*, *62*(10), 3379-3386.
9. Bousse, L., Van Den Vlekkert, H. H., & De Rooij, N. F. (1990). Hysteresis in  $\text{Al}_2\text{O}_3$ -gate isfets. *Sensors and Actuators B: Chemical*, *2*(2), 103-110.
10. Keeble, L., Moser, N., Rodriguez-Manzano, J., & Georgiou, P. (2020). ISFET-based Sensing and Electric Field Actuation of DNA for On-Chip Detection: A Review. *IEEE Sensors Journal*.
11. Sadighbayan, D., Hasanzadeh, M., & Ghafar-Zadeh, E. (2020). Biosensing based on field-effect transistors (FET): Recent progress and challenges. *TrAC Trends in Analytical Chemistry*, 116067.
12. Seo, G., Lee, G., Kim, M. J., Baek, S. H., Choi, M., Ku, K. B., ... & Kim, S. J. (2020). Rapid Detection of COVID-19 Causative Virus (SARS-CoV-2) in Human Nasopharyngeal Swab Specimens Using Field-Effect Transistor-Based Biosensor (vol 14, pg 5135, 2020). *ACS NANO*, *14*(9), 12257-12258.
13. Pankiew, A., Srisuwan, A., Thornyanadacha, N., Bunjongpru, W., & Ruangphanit, A. (2020, March). The Electrical Characterization of Nitride/Oxide Ion Sensitive Field Effect Transistor (NO-ISFET). In *2020 8th International Electrical Engineering Congress (iEECON)* (pp. 1-4). IEEE.
14. Evans, R. M., Balijepalli, A., & Kearsley, A. J. (2020). Transport Phenomena in Biological Field Effect Transistors. *SIAM Journal on Applied Mathematics*, *80*(6), 2586-2607.
15. Baldacchini, C., Montanarella, A. F., Francioso, L., Signore, M. A., Cannistraro, S., & Bizzarri, A. R. (2020). A Reliable BioFET Immunosensor for Detection of p53 Tumour Suppressor in Physiological-Like Environment. *Sensors*, *20*(21), 6364.
16. Chairirattanakua, W., Bunjongpru, W., Pankiew, A., Srisuwan, A., Jeamsaksiri, W., Chaowicharat, E., ... & Phromyothin, D. (2020). Modification of polyvinyl chloride ion-selective membrane for nitrate ISFET sensors. *Applied Surface Science*, *512*, 145664.
17. Lee, C. S., Kim, S. K., & Kim, M. (2009). Ion-sensitive field-effect transistor for biological sensing. *Sensors*, *9*(9), 7111-7131.
18. Jankovic, V., & Chang, J. P. (2011).  $\text{HfO}_2$  and  $\text{ZrO}_2$ -based microchemical ion sensitive field effect transistor (ISFET) sensors: simulation & experiment. *Journal of The Electrochemical Society*, *158*(10), P115.
19. Pachauri, V., & Ingebrandt, S. (2016). Biologically sensitive field-effect transistors: from ISFETs to NanoFETs. *Essays in biochemistry*, *60*(1), 81-90.
20. Kaisti, M. (2017). Detection principles of biological and chemical FET sensors. *Biosensors and Bioelectronics*, *98*, 437-448.

21. Qin, W., Beck, L. H., Zeng, C., Chen, Z., Li, S., Zuo, K., ... & Liu, Z. (2011). Anti-phospholipase A2 receptor antibody in membranous nephropathy. *Journal of the American Society of Nephrology*, 22(6), 1137-1143.
22. de Castro, L. S. O., de Moraes Cruz, C. A., Cardoso, V. F., da Silva, L. L. F., Pelegrini, M. V., & Marques, G. C. (2019, August). Improved ISFET Readout Circuit: Characterization and Comparison. In *2019 4th International Symposium on Instrumentation Systems, Circuits and Transducers (INSCIT)*(pp. 1-6). IEEE.
23. Yates, D. E., Levine, S., & Healy, T. W. (1974). Site-binding model of the electrical double layer at the oxide/water interface. *Journal of the Chemical Society, Faraday Transactions 1: Physical Chemistry in Condensed Phases*, 70, 1807-1818.
24. Bergveld, P. (1991). A critical evaluation of direct electrical protein detection methods. *Biosensors and Bioelectronics*, 6(1), 55-72.
25. Wrobel, G., Chalmel, F., & Primig, M. (2005). goCluster integrates statistical analysis and functional interpretation of microarray expression data. *Bioinformatics*, 21(17), 3575-3577.
26. Hoxha, A., Scarbolo, P., Cossettini, A., Pittino, F., & Selmi, L. (2016). ENBIOS-2D Lab, v1. 0.
27. Muhammad Asif, Muhammad Ajmal, Ghazala Ashraf, Nadeem Muhammad, Ayesha Aziz, Tayyaba Iftikhar, Junlei Wang, Hongfang Liu, (2020) The role of biosensors in coronavirus disease-2019 outbreak, *Current Opinion in Electrochemistry*, 23, 174-184.
28. Namrata Mendiratta, Suman Lata Tripathi, Sanjeevikumar Padmanaban and Eklas Hossain (2020) Design and Analysis of Heavily Doped n+ Pocket Asymmetrical Junction-Less Double Gate MOSFET for Biomedical Applications. *Applied Sciences*, 10 (7), 2499.
29. Suman Lata Tripathi, Raju Patel, Vimal Kumar Agrawal (2019) Low Leakage Pocket Junction-less DGTFT with Bio-Sensing Cavity Region. *Turkish Journal of Electrical Engineering and Computer Sciences*, 27(4), 2466-2474.

## Figures

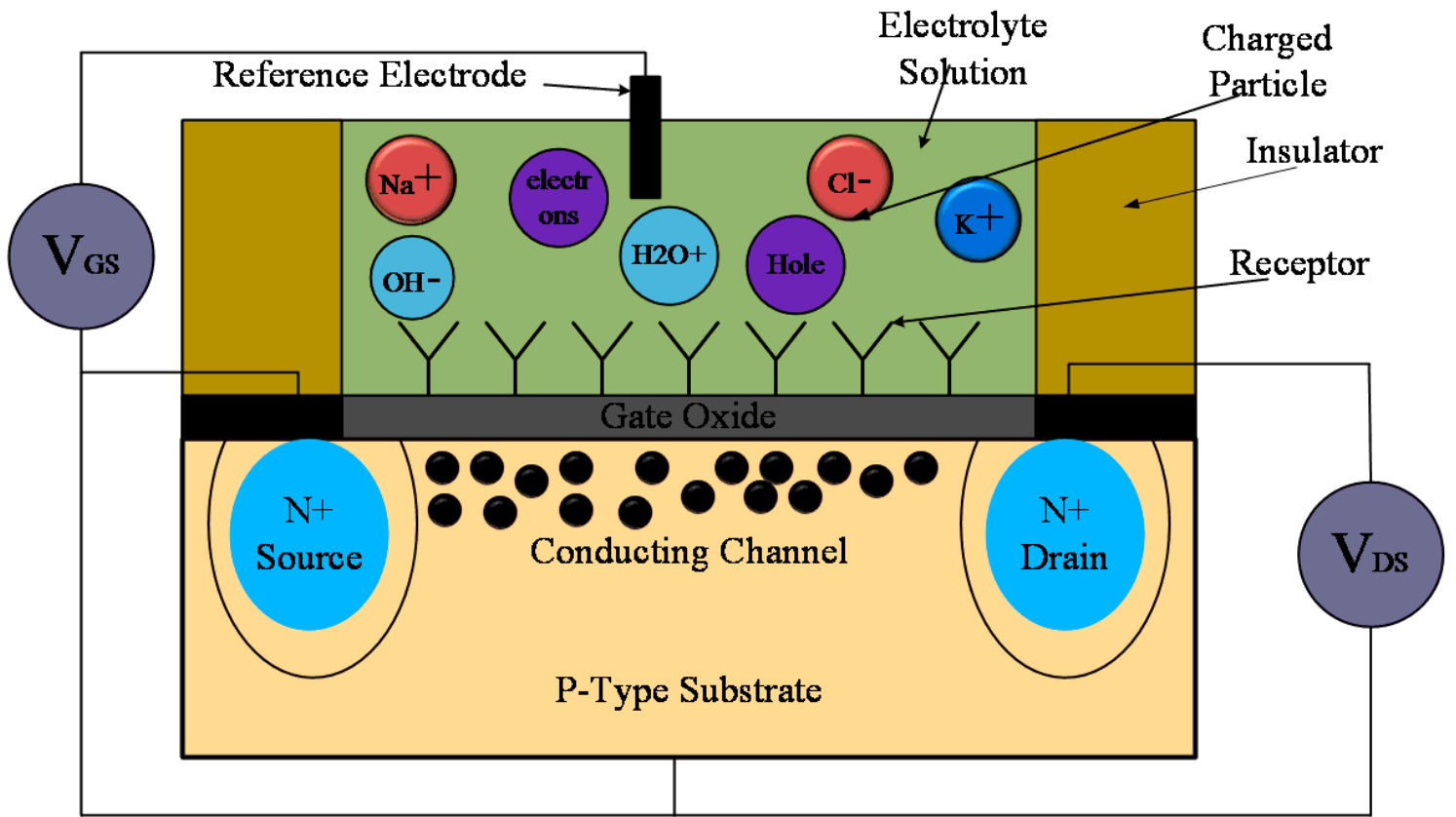


Figure 1

Ion Sensitive FET

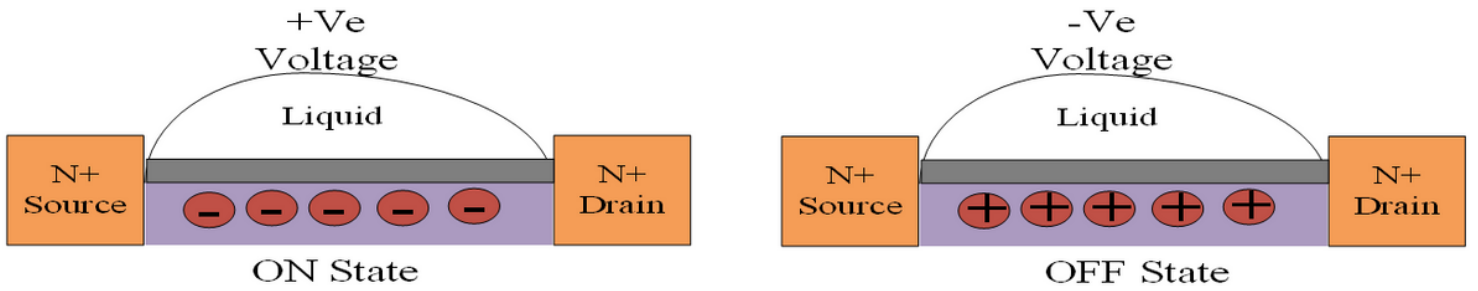


Figure 2

ON-OFF state of ISFET [22]

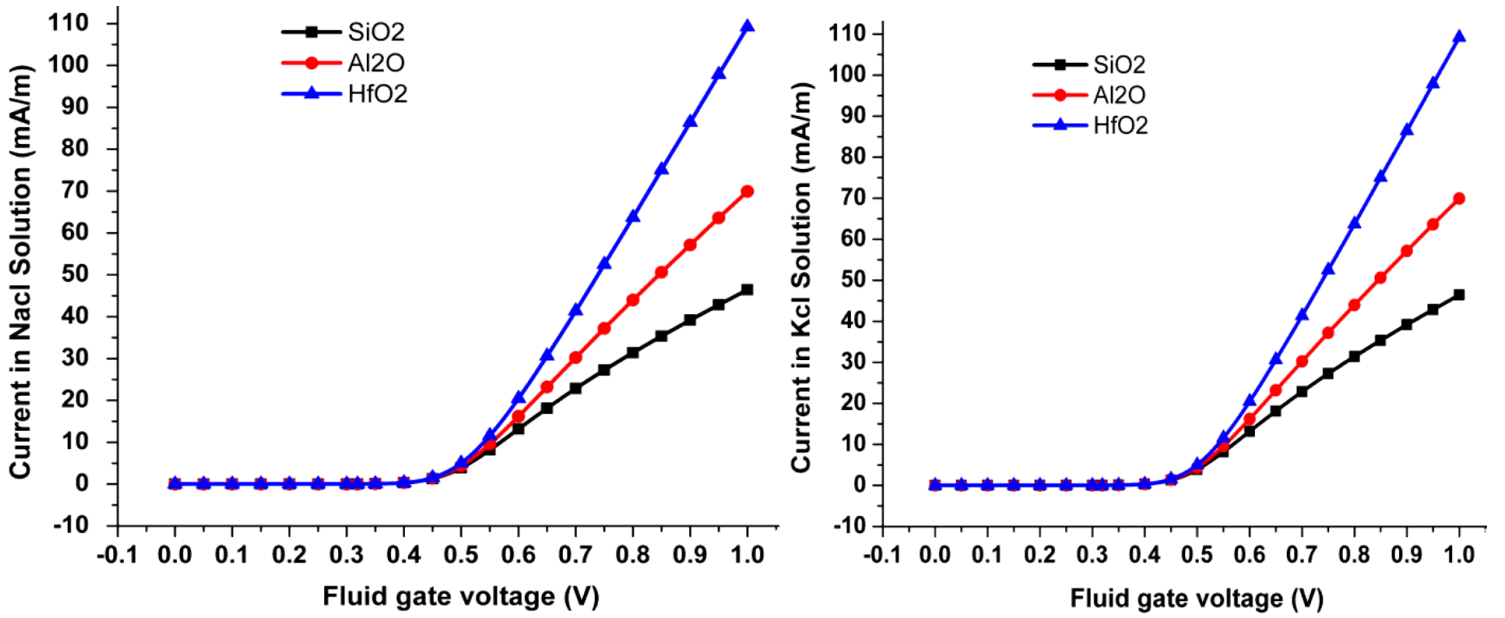


Figure 3

(a) Id-Vg in NaCl Solution (b) Id-Vg in KCl Solution

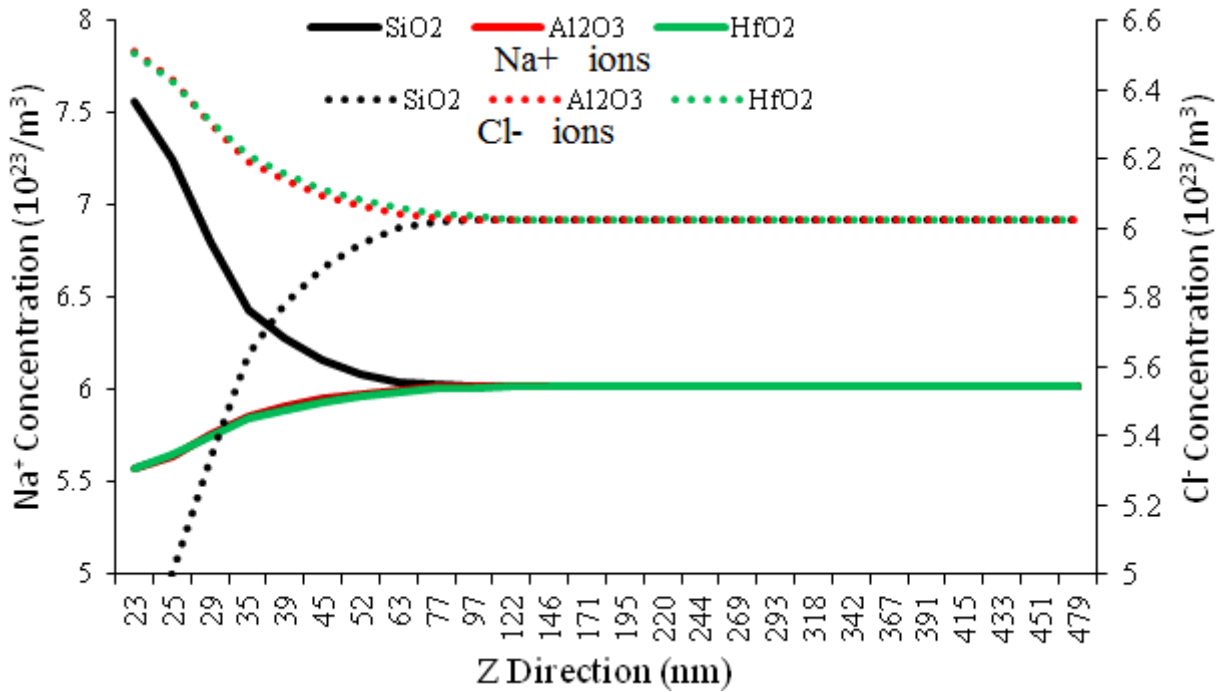


Figure 4

Concentration of Charged particle in NaCl Solution

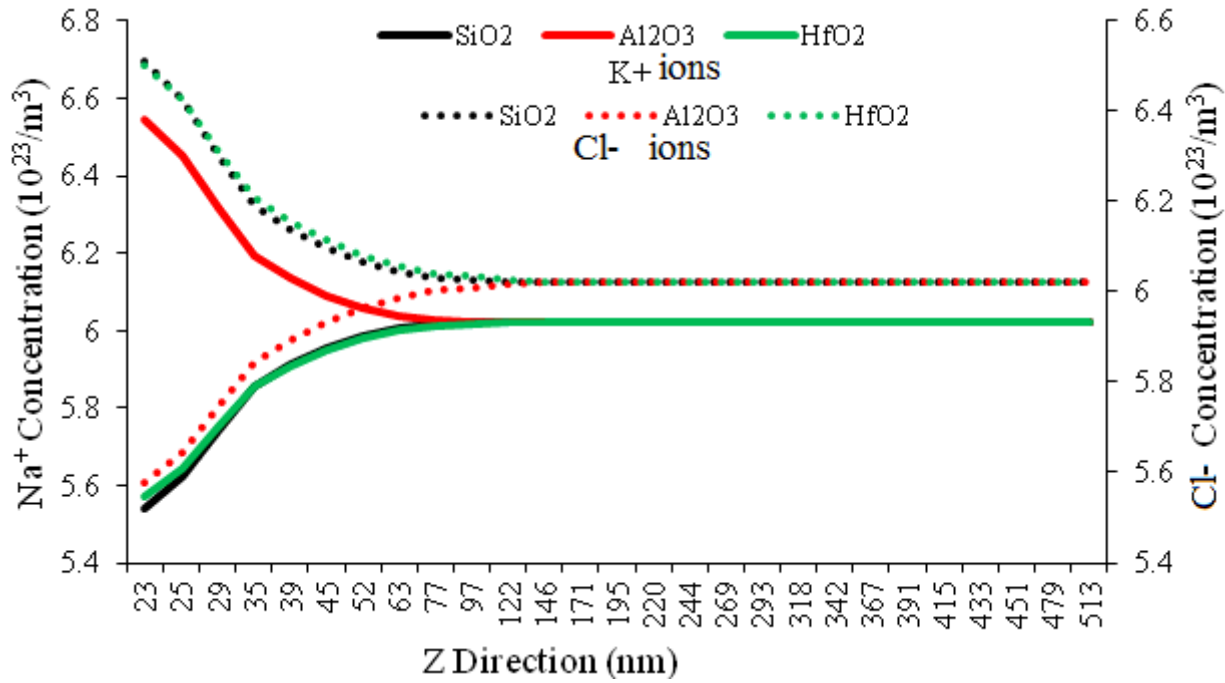


Figure 5

Concentration of Charged particles in KCL solution

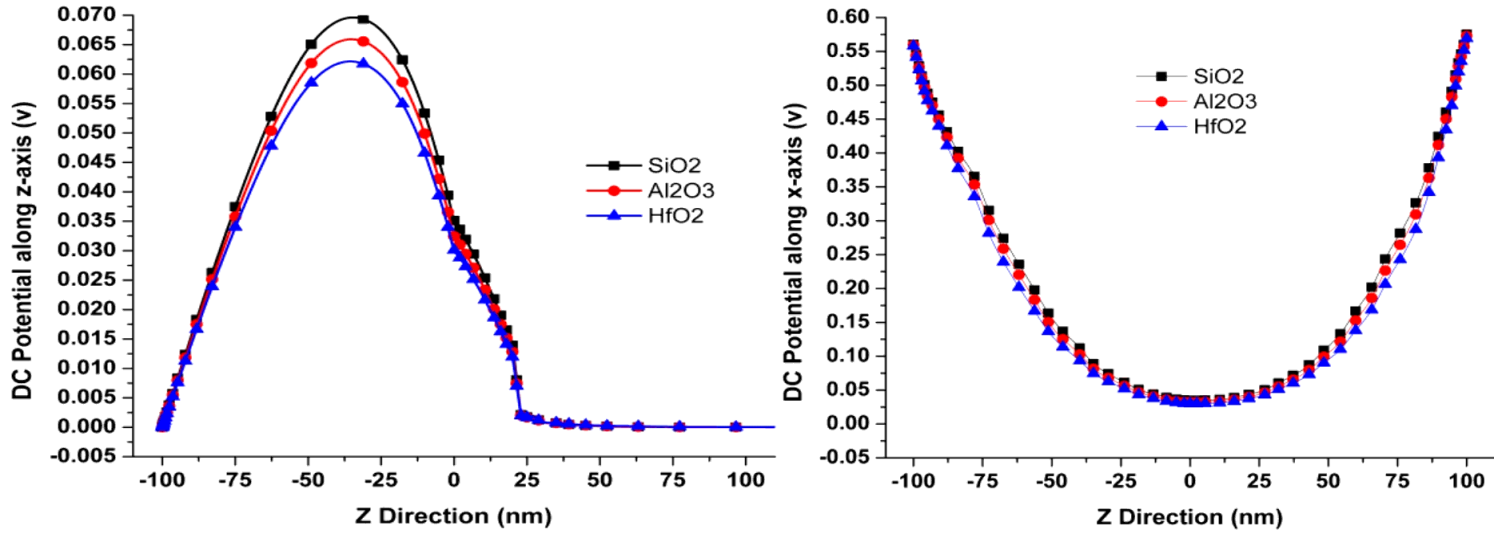
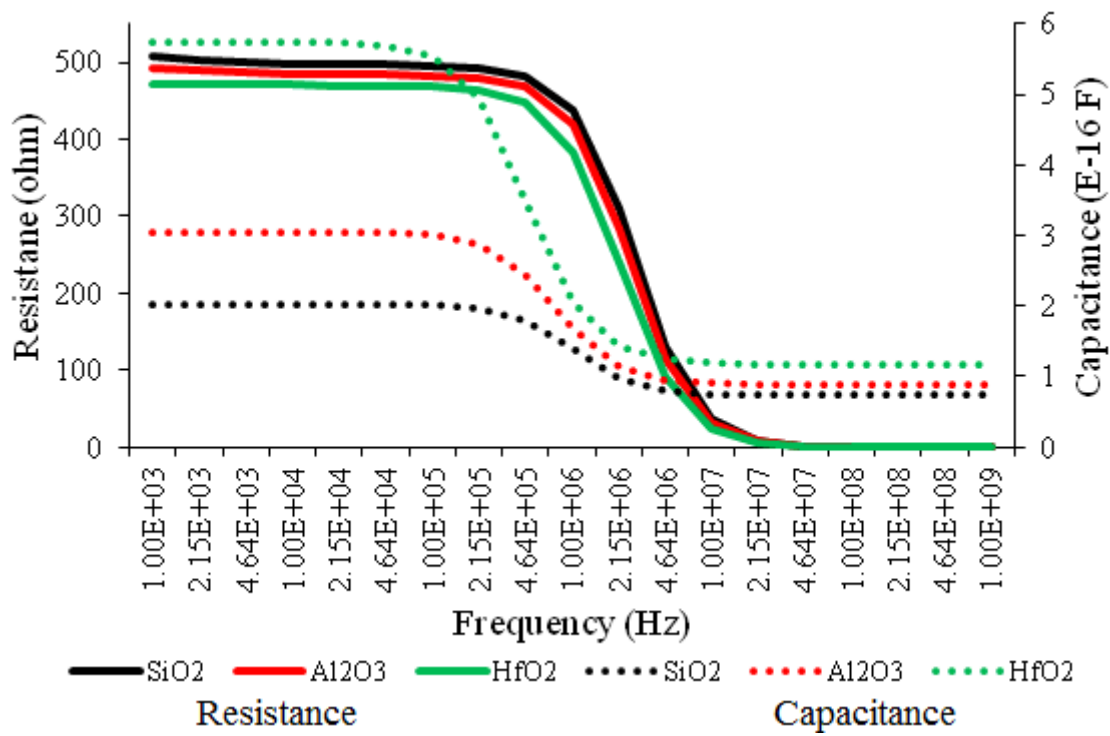


Figure 6

(a) DC potential along Z direction (b) DC potential along X-direction



**Figure 7**

Variation into Resistance and Capacitance in the channel of ISFET with different dielectric